LANGMUIR

pubs.acs.org/Langmuir Article

Membrane Cargo Density-Dependent Interaction between Protein and Lipid Domains on the Giant Unilamellar Vesicles

Juan Ureña, Ashlynn Knight, and Il-Hyung Lee*

Cite This: *Langmuir* 2022, 38, 4702−4712 Read Online

ACCESS | Metrics & More | Article Recommendations | Supporting Information

ABSTRACT: Protein cargos anchored on the lipid membrane can be segregated by fluidic domain phase separation. Lipid membranes at certain compositions may separate into lipid domains to segregate cargos, and protein cargos themselves may be involved in protein condensate domain formation with multivalent binding proteins to segregate cargos. Recent studies suggest that these two driving forces of phase separation closely interact on the lipid membranes to promote codomain formation. In this report, we studied the effect of cargo density on the outcome of the cargo phase separation on giant unilamellar vesicles. Proteins and lipids are connected only by the anchored cargos, so it was originally hypothesized that higher cargo density would increase the degree of interaction between the lipid and protein domains, promoting more phase separation. However, fluorescence image analysis on different cargo densities showed that the cooperative domain formation and steric pressure are at a tug of war opposing each other. Cooperative domain formation is dominant under lower anchor density conditions, and above a threshold density, steric pressure was dominant opposing the domain formation. The result suggests that the cargo density is a key parameter affecting the outcome of cargo organization on the lipid membranes by phase separation.

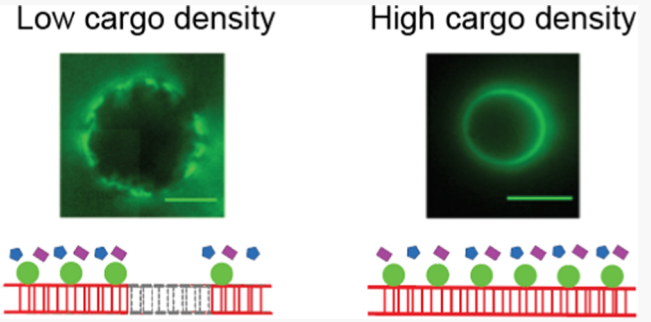

INTRODUCTION

Lipid membranes define the boundaries of cellular organelles. The organelles, including the nucleus, endoplasmic reticulum, mitochondria, lysosome, and plasma membranes, work as specialized spatial platforms to perform biochemical reactions in precisely coordinated timing. Membrane protein cargo sorting is a process where the spatiotemporal regulation of molecular organization is important. The process is necessary for successful vesicular trafficking between organelles, involving the spontaneous organization of cargo molecules, but its mechanism remains poorly understood. Thus, understanding the molecular mechanism of cargo protein organization on the lipid membranes is very important.

We used the reconstitution approach with synthetic systems.[1−13] Reconstitution approach is advantageous in the sense that researchers can test physical models in a well-defined environment that can inspire them to design and synthesize biomimetic systems for therapeutic purposes.[14−16] In this study, we used bottom-up reconstitution with giant unilamellar vesicle (GUV) system, a lipid bilayer vesicle with a typical diameter of 1−100 μm. GUV has a relatively well-defined lipid composition and can be readily observed by optical microscopy. We purified proteins to anchor one of them as cargo on the lipid membranes to study the organizational outcomes under different conditions. Lipids and proteins were fluorescently tagged to observe and quantify the outcome with fluorescence microscopy. We anchored fluorescent cargo proteins on synthetic vesicles at different surface densities and introduced a set of proteins capable of forming protein condensate or domains at high enough concentrations. The vesicles were ternary mixtures that domain-separate at low enough temperatures; thus, both proteins and lipids had their driving forces of domain separations. This report aims to specifically study the interaction between lipid and protein phase-separated domains on the lipid membranes at different protein cargo densities.

Lipid bilayer at different compositions shows various phase behaviors, such as gel-fluidic phase and miscibility transitions.[17,18] Fluidic domain separation is of particular importance when it comes to understanding the membrane organization of the plasma membrane.[19,20] Ternary mixture model lipid bilayers with unsaturated acyl chain lipids, saturated acyl chain lipids, and cholesterol can form distinct fluidic binary domains, namely, liquid ordered (lo) and liquid disordered (ld) domains.[18,21] Giant plasma membrane vesicles directly detached from the living cell plasma membranes were reported

Received: January 29, 2022
Revised: March 14, 2022
Published: April 6, 2022

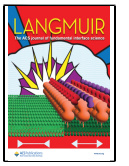

https://doi.org/10.1021/acs.langmuir.2c00247
Langmuir 2022, 38, 4702−4712

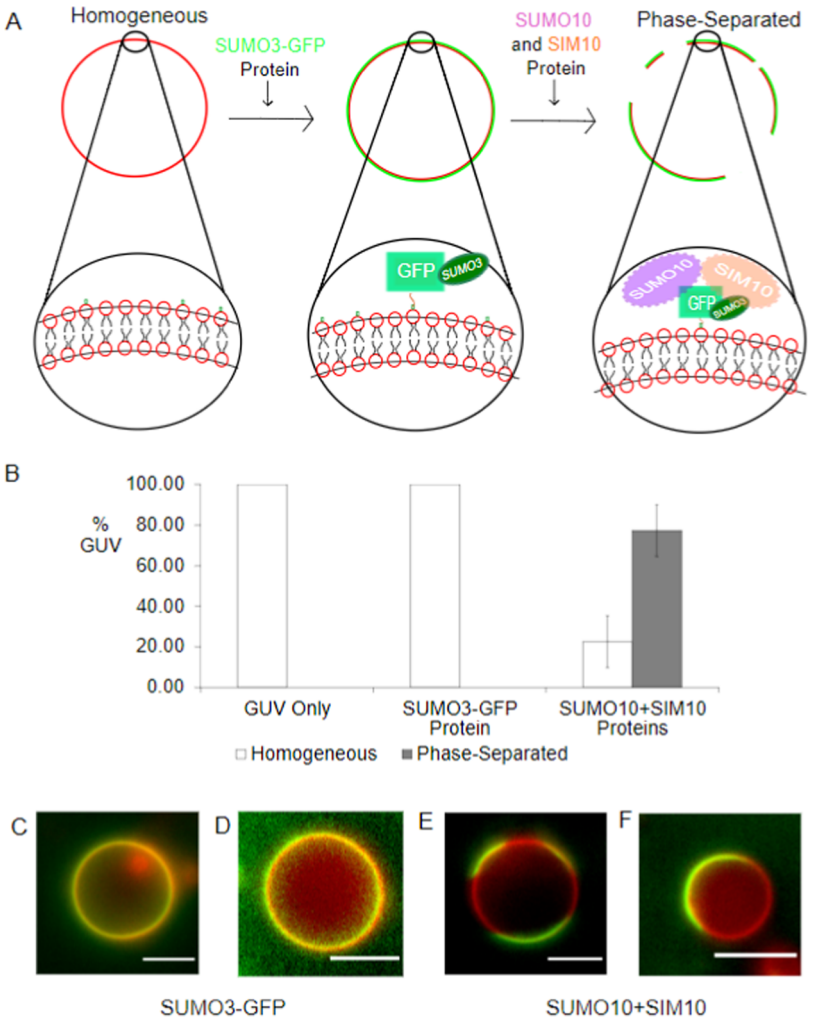

Figure 1. Homogeneous to phase-separated transition experiment with polySUMO−SIM proteins. (A) Schematic of the lipid−protein interaction of a 5% Ni-DGS GUV, transitioning from homogeneous to phase-separated after introducing SUMO3-GFP and polySUMO−SIM proteins. The lipid composition for homogeneous 5% Ni-DGS GUVs was DOPC 40%, DPPC 19.8%, cholesterol 35%, Ni-DGS 5%, and TR-DHPE 0.2%, and incubation conditions of the proteins were 1 μM SUMO3-GFP and 1 μM SUMO10 and SIM10 each. (B) Statistical distribution of the resulting phase behavior of GUVs. The ratio of phase-separated GUV increased after introducing 1 μM SUMO3-GFP and 1 μM polySUMO−SIM proteins. (C, D) Example images of GFP cargo fluorescence (green) overlapped with Texas Red lipid fluorescence (red), maintaining homogeneous behavior after introducing SUMO3-GFP protein. (E, F) Example images showing phase-separated behavior after introducing polySUMO−SIM proteins. Scale bars are 5 μm.

to exhibit a similar domain separation behavior.[22−24] However, in living cells, such domain separation exists at a much smaller scale and is more dynamic[25−28] with some notable exception cases.[29,30] The physiological lipid domains are often referred to as lipid rafts[31,32] that are involved in various cellular activities.[33−36] As different molecules will have different partitioning behaviors in the raft domains,[37−39] lipid rafts can play the functional role as a molecular sorting platform. More recently, another biological domain formation that has become an important topic is liquid−liquid phase separation (LLPS) of proteins. Proteins with multivalent binding capability or intrinsically disordered domains at high enough concentrations can form colloid-like droplets in solutions.[40−43] The droplets can segregate cargo proteins inside,[44,45] and it is becoming evident that many membrane-less organelles are maintained by forming such protein domains.[46−48] When such protein domain formation occurs on the lipid membrane by one of the protein components being a membrane protein, membrane-specific protein domain formation occurs. Example systems include T-cell receptor,[49−51] synaptic density,[52,53] nephrin,[54] and tight junction.[55] What requires more investigation is the outcome of coexisting driving forces of lipid-driven and protein-driven domain formations on the membrane. Previous studies have shown that these two driving forces tend to work cooperatively to form coupled codomain when the lipid bilayer and membrane protein can exhibit domain separation behavior.[1,56] In most cases, proteins can interact with lipid membranes only through membrane-anchored proteins, so it is interesting to study the outcome of the interaction between the two driving forces of lipid and protein domain formations at different anchor densities. We report a quantitative case study on the topic of anchored protein density-dependent outcome of the interaction between lipid and protein domains on lipid membranes, specifically using three-component protein systems that form fluidic protein domains with one of the three components anchored to the lipid membrane that we call cargo proteins.

https://doi.org/10.1021/acs.langmuir.2c00247
Langmuir 2022, 38, 4702−4712

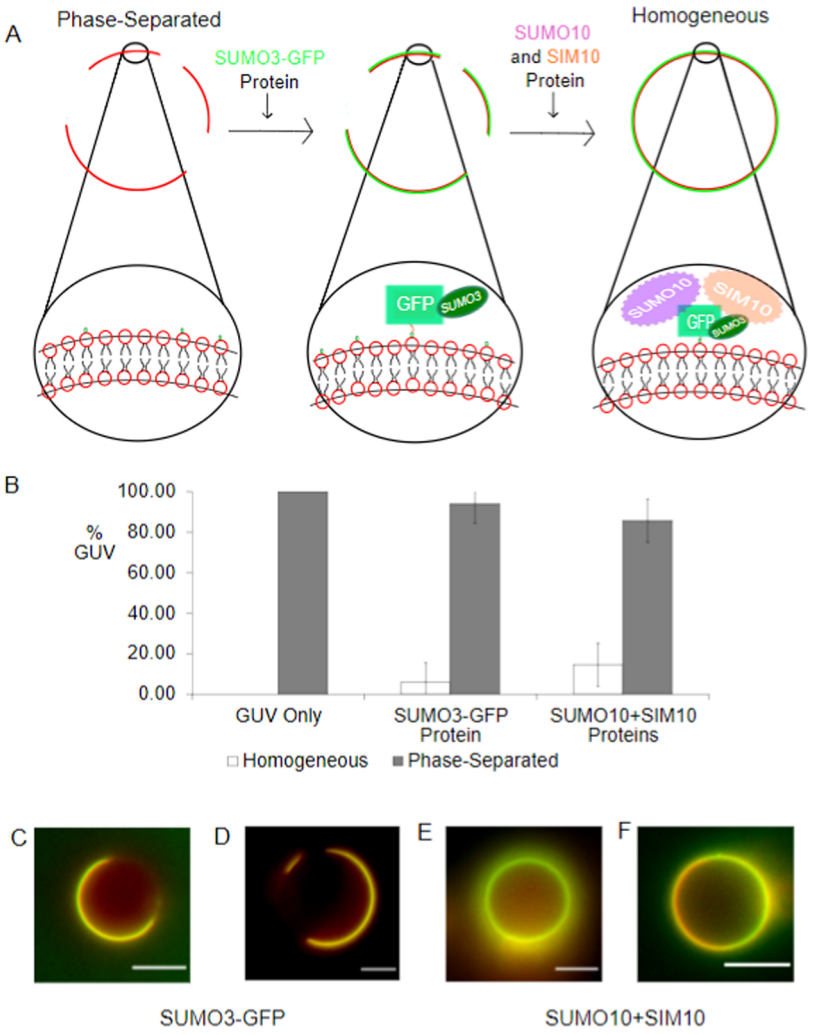

Figure 2. Phase-separated to homogeneous transition experiment with polySUMO−SIM proteins. (a) Schematic of the lipid−protein interaction of a 5% Ni-DGS GUV, transitioning from phase-separated to homogeneous after introducing SUMO3-GFP and polySUMO−SIM proteins. The lipid composition of the phase-separated 5% Ni-DGS GUVs was DOPC 30%, DPPC 39.8%, cholesterol 25%, Ni-DGS 5%, and TR-DHPE 0.2%, and incubation conditions of the proteins were 1 μM SUMO3-GFP and 1 μM SUMO10 and SIM10 each. (B) Statistical distribution of pre-existing lipid domains transitioning into the homogeneous state. The ratio of homogeneous GUV increased after introducing 1 μM of SUMO3-GFP and 1 μM of polySUMO−SIM proteins. (C, D) Example images of GFP cargo fluorescence (green) overlapped with Texas Red lipid fluorescence (red), maintaining phase-separated behavior after introducing SUMO3-GFP protein. (E, F) Example images showing homogeneous behavior after introducing polySUMO−SIM proteins. Scale bars are 5 μm.

RESULTS AND DISCUSSION

Membrane-Anchored Cargo Proteins Mediate Cooperative Cargo Domain Formation. We used the ternary lipid mixture GUV and poly small ubiquitin-like modifier (SUMO)−SUMO interacting motif (SIM), polySUMO−SIM proteins as our model system. Ternary lipid mixture membranes with saturated acyl chain lipids, unsaturated acyl chain lipids, and cholesterol form fluidic lo and ld domains under certain conditions.[18,21,57,58] polySUMO−SIM protein system is an artificially constructed system by the Rosen group that forms LLPS protein droplets.[44,59] The system preferentially recruits SUMOylated cargos inside the protein droplet domains. We originally hypothesized that ternary lipid mixture membranes and multicomponent protein systems with LLPS behavior, when interacting on the lipid membrane, will always enhance the probability of creating codomain (domains formed as a collaborative interaction between lipid and protein domains), and higher anchoring density of proteins on the membrane will further promote the codomain formation. This hypothesis was inspired by the fact that lipids and proteins mostly interact through the anchored proteins, and having more anchored proteins will increase the amount of interaction.[1] To test the hypothesis, we designed a serial lipid−protein interaction experiment, as shown in Figure 1A. Ternary mixture lipid GUVs with fluorescent lipid reporters were prepared. The lipid composition was 1,2-dioleoyl-*sn*-glycero-3-phosphocholine (DOPC) 40%, 1,2-dipalmitoyl-*sn*-glycero-3-phosphocholine (DPPC) 19.8%, cholesterol 35%, 1,2-dioleoyl-*sn*-glycero-3-[(*N*-(5-amino-1-carboxypentyl) iminodiacetic acid)succinyl] (Ni-DGS) 5%, and Texas Red-1,2-dihexadecanoyl-*sn*-glycero-3-phosphoethanolamine (TR-DHPE) 0.2%. After initial characterization by fluorescence imaging, SUMO3-green fluorescence protein (SUMO3-GFP), a membrane cargo protein to be lipid-anchored via coordination bonding between His-tag and Ni-DGS lipids (5% by mol composition), was introduced. Enough incubation time allowed cargo proteins to fully anchor to the lipid

https://doi.org/10.1021/acs.langmuir.2c00247
Langmuir 2022, 38, 4702−4712

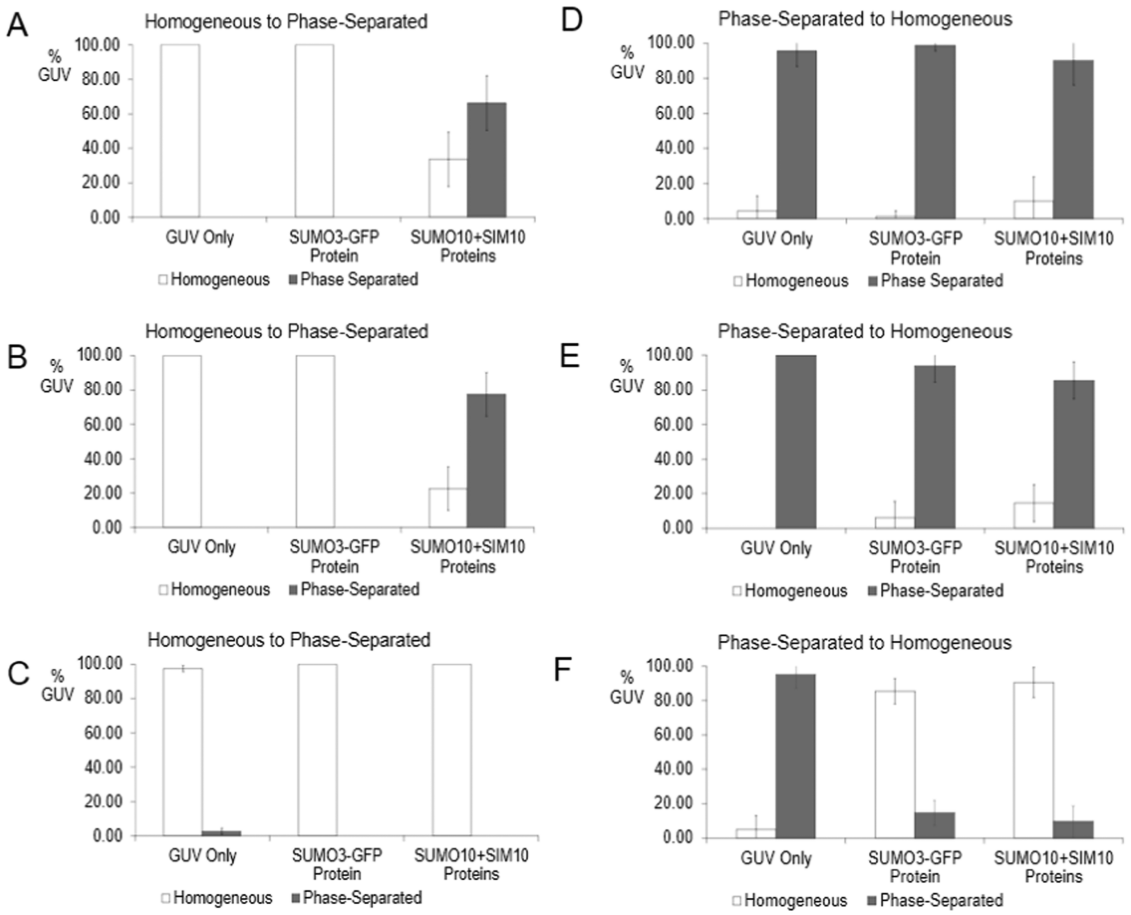

Figure 3. Statistical distribution for protein density sweeping experiments at various lipid composition GUVs. (A−C) Statistical distribution of the states for initially homogeneous GUVs with 2.5% (A), 5% (B), and 10% (C) Ni-DGS concentrations, respectively. Ni-DGS replaced DOPC to match the acyl chain property. In 2.5 and 5% Ni-DGS concentrations, an increase in phase-separated GUVs was observed after introducing polySUMO−SIM proteins. Vesicles remained homogeneous in all conditions in 10% Ni-DGS concentration. (D−F) Statistical distribution for initially phase-separated GUVs with 2.5% (D), 5% (E), and 10% (F) Ni-DGS concentrations. Ni-DGS replaced DOPC to match the acyl chain property. In 2.5 and 5% concentrations, a small increase in homogeneous GUVs was observed after introducing SUMO3-GFP and polySUMO−SIM proteins. In 10% Ni-DGS concentration, a substantial increase was observed after introducing SUMO3-GFP and polySUMO−SIM proteins.

membranes at 1 μM concentration. After imaging the protein-bound vesicles, two additional polySUMO−SIM proteins, SUMO10 and SIM10, 1 μM each, were added, triggering multivalent interactions between proteins. Fluorescence images were statistically analyzed to count the ratio of vesicles with clearly visible domains on the membranes.

As shown in Figure 1B, ternary lipid vesicles at mostly homogeneous or uniform states maintained their state after binding the SUMO3-GFP cargo proteins at 100% by population distribution of vesicles. When a full set of polySUMO−SIM proteins were introduced, the state distribution was shifted toward the phase separation or domain formation, decreasing the population of the homogeneous vesicles to 20%. Figure 1C−F shows example fluorescence images of SUMO3-GFP distribution at different states. It suggests that the polySUMO−SIM protein caused membrane protein cargos to be segregated into domains. It further validates the previous experimental observations in other protein systems that lipid membranes with phase separation properties and proteins with phase separation properties tend to cooperatively form coupled domains.[1,56] GUVs with no functional lipids do not interact with the proteins (Supporting Materials Figure S1), which suggests that the interaction is mediated by the anchored cargo SUMO3-GFP.

High Surface Density of Protein Domains Reverses the Pre-Existing Domains. To test our original hypothesis of higher lipid-anchored cargo density further promoting more domain formation on the lipid membrane, we performed related experiments to Figure 1 with higher densities of lipid anchors. However, the outcome was inconsistent with the original hypothesis. Instead, we learned that higher anchor density resulted in the opposite effect of reversing the even pre-existing lipid domains into the homogeneous state. Figure 2 shows the similar schematic, statistical analysis, and example images to Figure 1 for the experiments on ternary mixture membrane with a composition of pre-existing phase separation (DOPC 30%, DPPC 39.8%, cholesterol 25%, and -DHPE 0.2% with the same 5% Ni-DGS anchor mol composition). SUMO3-GFP and polySUMO−SIM proteins were added sequentially in the same concentration and incubation conditions used in Figure 1.

According to the data in Figure 2, the originally phase-separated GUVs slightly increased in the ratio of vesicles with a homogeneous state from 0 to 5% after binding the SUMO3-GFP cargo proteins. When the complete set of polySUMO−SIM proteins was introduced, more vesicles became homogeneous, losing the pre-existing domains and increasing the homogeneous vesicle ratio up to about 15%. Even though most

https://doi.org/10.1021/acs.langmuir.2c00247
Langmuir 2022, 38, 4702−4712

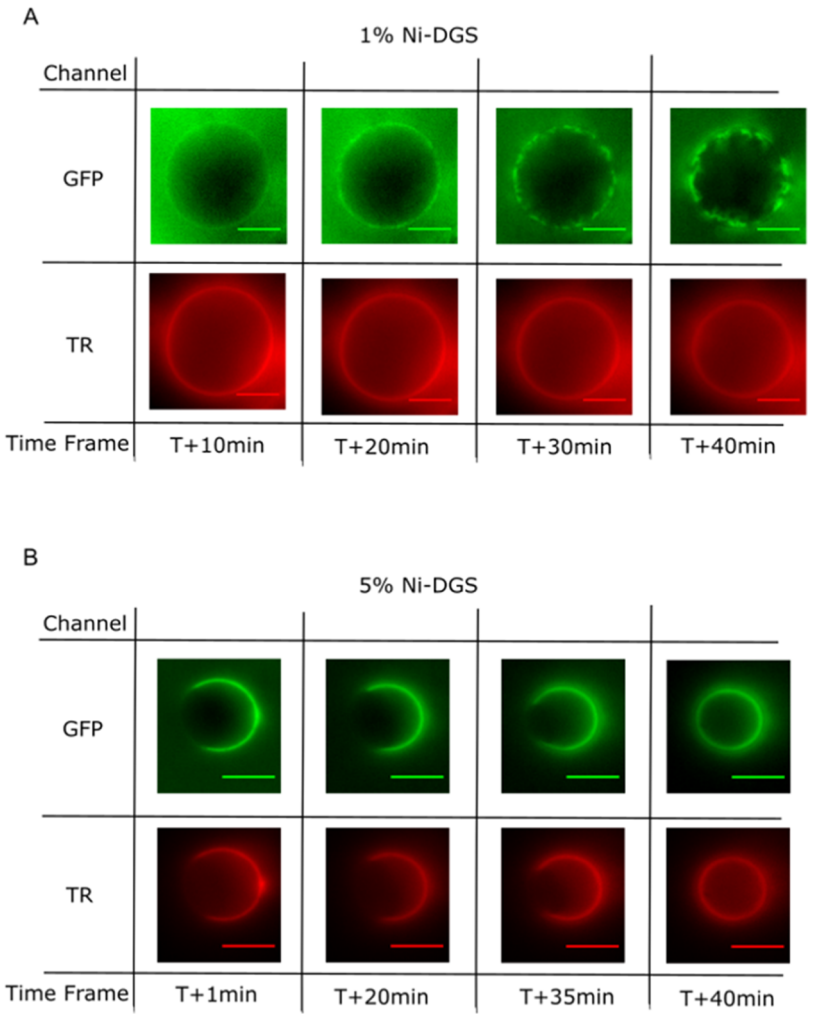

Figure 4. Time-lapse images of GUVs changing states from homogeneous to phase-separated and phase-separated to homogeneous. (a) GUVs changing from homogeneous to phase-separated in a time lapse of +10, 20, 30, and 40 min. Images were collected in the GFP fluorescence channel represented in green and Texas Red fluorescence channel represented in red. (b) GUVs change from phase-separated to homogeneous in a time lapse of +10, 20, 30, and 40 min. Images were collected in the GFP fluorescence channel represented in green and Texas Red fluorescence channel represented in red. Scale bars are set to 5 μm.

vesicles remained phase-separated toward the end, the increased homogeneous population could not be missed. It means that the high lipid anchor density opposed the cooperative domain formation and pushed the state population toward the homogeneous state instead of promoting phase separation. It suggests that cooperative interaction between the driving forces of lipid and protein domain formations on the lipid membranes does not simply increase as a function of anchoring density, and there is another opposing force against the domain formation that becomes dominant at higher anchoring density.[60,61]

Cargo Density Dependence Study Suggests a Tug of War between Cooperative Domain Formation and Steric Pressure of Membrane Protein Cargo Crowding. We conducted a systematic anchor density sweeping study on ternary mixture lipid vesicles with mostly phase-separated and homogeneous states to rationalize the trend. GUVs with different lipid anchor densities of 2.5, 5, and 10% mol compositions of Ni-DGS were serially incubated with SUMO3-GFP cargo followed by a set of polySUMO−SIM proteins. To ensure the same ratio of saturated and unsaturated lipids, the difference in Ni-DGS was replaced by the DOPC, identical acyl chain lipids. Fluorescence images of many samples were taken at each stage, and statistical analysis was performed to quantify the phase separation state.

As shown in Figure 3A−C, initially homogeneous lipid vesicles (similar to Figure 1) all retained the state after binding to the SUMO3-GFP cargo proteins. When the full set of polySUMO−SIM proteins was added, the population distribution shifted toward phase separation, reversing the major population for lipid anchor density of 2.5 and 5%, suggesting the effect of cooperative domain formation between lipids and proteins. When the anchor density was as high as 10%, this cooperative domain formation was no longer observed, and the vesicles remained mostly homogeneous even after introducing the polySUMO−SIM proteins. As shown in Figure 3D,E, initially phase-separated lipid vesicles (similar to Figure 2) slightly increased the population of homogeneous vesicles when SUMO3-GFP cargos and polySUMO−SIM were added for anchor densities of 2.5 and 5%, while most vesicles remained phase-separated. This was dramatically different when the anchor density was as high as 10%, as shown in Figure 3F. Most vesicles became homogeneous after binding to the SUMO3-GFP cargo proteins, and adding polySUMO−

https://doi.org/10.1021/acs.langmuir.2c00247
Langmuir 2022, 38, 4702−4712

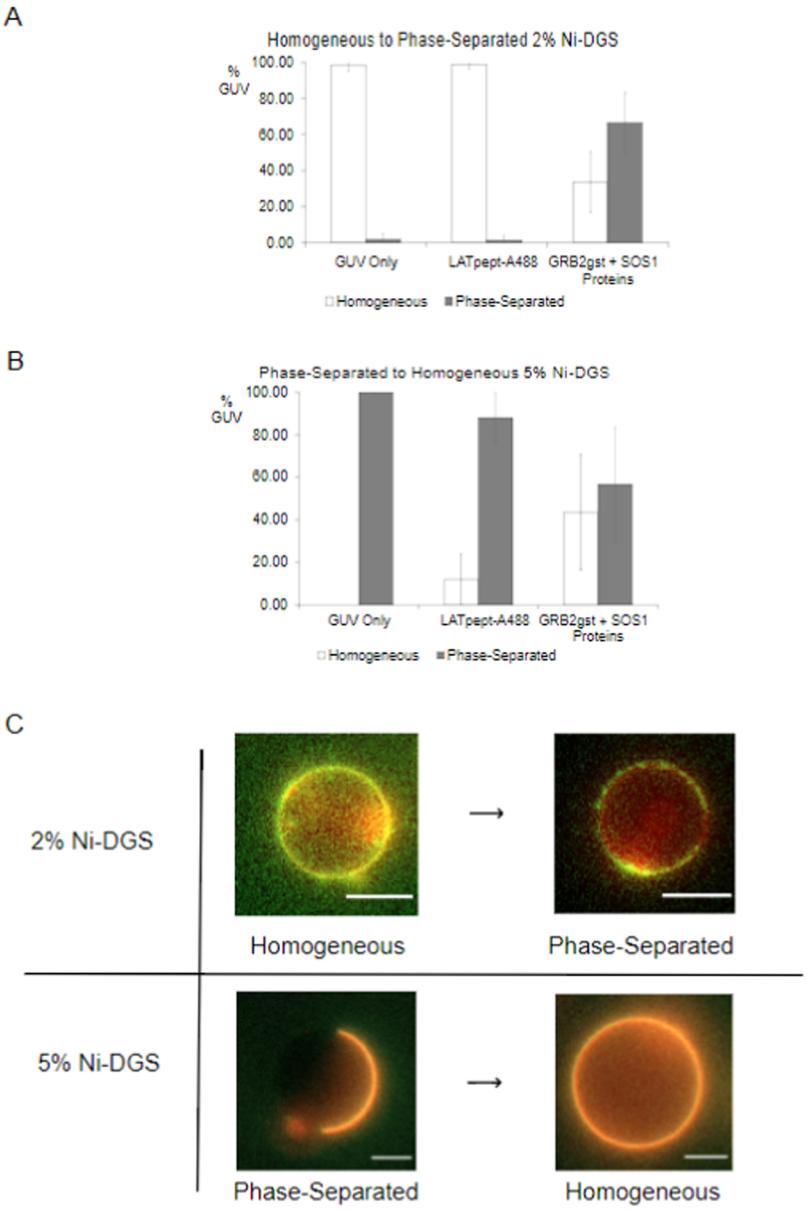

Figure 5. Summary of the LATpept/GRB1/SOS1 protein experiment. (A) Statistical distribution of the resulting phase behavior of 2% Ni-DGS GUV. After introducing LATpept, GRB2, and SOS1 proteins, an increase in phase-separated GUV was observed. (B) Statistical distribution of pre-existing lipid domains into a homogeneous state of 5% Ni-DGS GUV. After introducing LATpept, GRB2, and SOS1 proteins, an increase in the homogeneous GUV was observed. (C) Example images of 2% Ni-DGS and 5% Ni-DGS GUVs transitioning phase states after introducing LATpept, GRB1, and SOS1. LATpept was labeled with Alexa488 (green), and Texas Red was used for lipids (red). Scale bars are 5 μm.

SIM protein only promoted the trend toward the homogeneous state further by a few percent instead of phase-separating it. Overall, for the polySUMO−SIM system interacting with the ternary mixture lipid membrane system at two different compositions with different initial states, 10% Ni-DGS was the threshold anchor density, below which the driving force of cooperative domain formation[1,56] and steric pressure of membrane cargo molecules[60,61] were in balance mostly favoring the phase-separated state. Steric pressure means the repulsion of crowded cargo molecules, and the Stachowiak group characterized the effect of steric pressure on pre-existing lipid domains.[60−62] At the threshold composition of 10% Ni-DGS, the system largely favored the homogeneous state even after binding the SUMO3-GFP cargo, and adding polySUMO−SIM proteins did not reverse the trend, as is the case for lower anchor density vesicles. This trend shows that there is a threshold anchor density, above which the steric pressure-driven homogeneous state is largely favored and below which the cooperative coupled domain formation is favored.

Dynamic Aspect of the State Change. After fully incubating the systems to stabilize the state, all statistical analysis for the domain separation state was performed for the end results before making a quantitative observation so far. We also conducted time lapse of the state changes to monitor how the changes occur in real time for vesicles going through the transition. Figure 4A shows example time-lapse images of a vesicle with an initially homogeneous state changing from SUMO3-GFP cargo-bound homogeneous state to a phase-separated state after the full addition of polySUMO−SIM proteins. As shown in the example, the homogeneous

https://doi.org/10.1021/acs.langmuir.2c00247
Langmuir 2022, 38, 4702−4712

distribution of cargo proteins goes through a gradual decomposition of fluidic phase separation as a function of time.[40,50,54] Separated domains eventually matured and coarsened to show nearly complete binary segregation on the membranes. This is an expected behavior for fluidic domain formation on the membranes.[63,64] When we simultaneously analyzed the matching fluorescence from the lipid fluorescence, it was learned that the lipid channel in most cases did not exhibit enough contrast via TR-DHPE between two domains when domain separation occurred. Previous studies on related systems showed that lipid and protein domains showed enough contrasts to be distinguished by the confocal fluorescence intensity difference in the case of cooperative domain formation.[1,56] It possibly suggests that lipid partitioning behavior into cooperatively separated codomain may not be identical in all membrane protein systems, and codomain formation does not necessarily recreate the identical partitioning preferences observed in pure lipid-driven domains.[22,58]

Figure 4B shows an example time-lapse image for the case of initially phase-separated vesicles after binding to SUMO3-GFP cargo protein transitioning into a homogeneous state after adding polySUMO−SIM proteins. As shown in the time-lapse image, domains grew in the original cargo protein sparse (dark) region maintaining the cargo protein-rich domain (bright), suggesting that the steric pressure of additional interaction enlarged the domain coverage area. When matching fluorescence images of the lipid channel were analyzed, it was evident that lipid fluorescence closely followed the growth of the protein domain, suggesting coupled codomain growth. When the colocalization of the three participating proteins, SUMO3-GFP, SUMO10, and SIM10, was studied using the three-color label experiments, these proteins showed complete colocalization in both homogeneous and domain-separated states (Supporting Materials Figure S3).

Tug of War Is a Common Property of a Three-Component Protein System with Liquid-like Domain Formation. As more research reports are published on the topic of LLPS or colloidal droplet domain formation of proteins, it is becoming evident that there is a general group of proteins that can form droplets, such as multivalent binding proteins and intrinsically disordered proteins. What is also becoming clear is that each protein droplet system has its physical properties that is different from other systems. For example, some protein droplets behave like fluidic phases but some are like relatively rigid gels or complete solids.[65] The same protein system may be at various states depending on the physical condition necessitating characterization of the phase diagram as a function of various physical parameters.[66−68] To avoid jumping into the unjustified generalization of the phenomenon, we also performed the experiments with a similar protein system, specifically linker for activating T-cell peptide (LATpept)−growth factor receptor-bound protein 2 (GRB2)−Son of sevenless 1(SOS1) protein system.[49−51] This is a very similar system to the SUMO3-GFP and polySIM−SUMO system[44] because both are three-component systems with one of three that is mostly responsible for mediating the lipid−protein interaction by being anchored to the membranes and three at a sufficiently high protein concentration that can form protein droplet with liquid-like fluidity.

Figure 5 shows the sequential incubation experiments on the ternary mixture membrane system with LATpept−GRB2−SOS1. GUVs with the initial condition of homogeneous state and phase-separated state each were incubated with a fluorescently tagged (Alexa488) LAT peptide followed by a full set of GRB2 and SOS1 proteins. At a low anchoring density of 2% Ni-DGS, initially homogeneous vesicles became phase-separated when all proteins interacted, reversing the major population. At a higher anchoring density of 5% Ni-DGS, initially phase-separated vesicles became gradually homogeneous as more proteins were added sequentially. This shows that the observation of tug of war between cooperative domain formation and steric pressure applies to this similar but unrelated system, proving that the same driving force governs similar systems. What is notable is that the threshold mol % composition for LAT−GRB2−SOS1 was only 5%, while it was 10% for the polySUMO−SIM system, possibly due to the higher steric pressure of bigger cargo proteins. Additionally, a gradual increase in the homogeneous state vesicles in sequential addition is more obvious in LAT−GRB2−SOS1 experiments. It shows that the protein domain formation can further contribute to the increased cargo crowding on the membranes. Dynamic state change of the LAT−GRB2−SOS1 systems showed a similar behavior to the polySUMO−SIM system of Figure 4(Supporting Materials Figure S2).

Descriptive Model of the Cargo Density Dependence. For the systems we studied in this report, we did not find a single case where lipid membrane and membrane-anchored protein domains formed independently on the membrane space, such as the mismatched location of two domains on the same vesicle. Therefore, we categorized the outcome of our observation as cargo homogeneous state and cargo domain-separated state. Our observation can be described by a tug of war between two contributions of cooperative domain formation, favoring the cargo phase-separated state,[1,31,56,69] and steric pressure of cargo proteins on the membranes, favoring the cargo homogeneous state,[60,61] as shown in Figure 6. The driving force of codomain formation promotes a cargo phase-separated state, and the driving force of steric pressure promotes a cargo homogeneous state, thus competing for the final outcome. The influence of codomain formation is expected to increase as a function of anchoring density because the anchoring lipid is the mediator between the proteins and lipids. However, the absolute magnitude of the steric pressure also increases as a function of anchoring density because the degree of molecular crowding increases when there is a higher density of proteins in the limited space on the membranes.[60,61] When we treat these two contributions

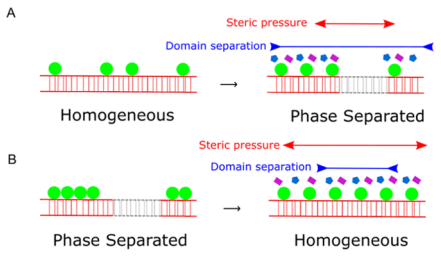

Figure 6. Schematic illustration of the interaction between the driving forces of domain separation and opposing steric pressure. (A) When cooperative domain separation dominates, the cargo proteins are phase-separated from the original homogeneous state. (B) When molecular steric pressure dominates, originally phase-separated cargo molecules become homogeneously distributed.

https://doi.org/10.1021/acs.langmuir.2c00247
Langmuir 2022, 38, 4702−4712

independently, our observation suggests that the contribution of the steric pressure increases more sharply above a certain protein cargo density on the membrane, making the steric pressure dominant at densities above the threshold density. This trend can never be reversed by the contribution of the codomain formation even though its absolute magnitude will presumably also increase at a higher protein density. This is a relatively simple rationalization based on the observation, but it concisely summarizes our experiments based on two well-known driving forces of the system.

What is lacking in the simple descriptive model is molecular detail. Our previous report suggested a double-layered Ising model as a simulation model to explain the cooperative domain formation between lipid membranes and anchored proteins.[1] Lattice model proteins anchored to the Ising model capture further details of expected behavior in various cases of proteins wetting the lipid membranes where the proteins closely interact with the membranes.[69] Introducing steric disadvantage between membrane protein cargos (anchors) in the double-layered two-dimensional (2D) Ising model reproduced our observation to some degree (Supporting Materials Figure S4). Still, the model is limited to the capacity of explaining the observed ensemble outcome based on the interaction of binary domains. The driving force of binary domain separation in our experiment is a result of at least three molecules interacting with each other in both lipid[70] and protein domains. Thus, details of the molecular interaction leading to the close interaction between lipid and protein domains deserve more investigation.

Another important point to consider is that regardless of the driving forces that led to the formation of the membrane-specific protein condensate domains, our experiments technically cannot distinguish the cargo homogeneous state by completely dissolved cargo proteins (noncondensate state) and cargo homogeneous state by domain area expanded to cover the entire membrane surface (maintained condensate state). Considering that the maximum 10 mol % anchoring lipid was used, complete coverage by the protein condensate means the significant area covered by the condensate structure. However, due to the lack of such measures on the condensate's molecular area occupied on the membrane, we cannot conclude definitely. Future studies on molecular details using atomic force microscopy may distinguish the molecular state of the final outcome.

In our experiment, we varied the mol % of the functionalization lipid, Ni-DGS, to vary the surface density of the protein cargo molecules, but it is possible that the mol % of the functionalization lipid is not linearly proportional to the final amount of cargo proteins anchored. To systematically quantify the amount of proteins anchored at different functionalization lipid concentrations, we conducted fluorescence intensity quantification at different mol % of the functionalization lipid (Supporting Materials Figure S5). The data show a significant difference in the amount of cargo protein anchored between the mol % of 2.5, 5.0, and 10.0% of Ni-DGS we used in the experiments, suggesting that the general trend observed was truly the outcome of the difference in membrane cargo density.

CONCLUSIONS

We studied protein cargo density-dependent phase separation state change on GUVs by bottom-up reconstitution and fluorescence imaging. Ternary mixture GUVs and three-component protein systems with known domain separation properties were used to study their cooperative phase behavior when cargo protein was anchored to the membrane bridging the driving forces of lipid-driven and protein-driven phase separations. Our observation suggests that proteolipid systems tend to cooperatively form cargo domains when anchor density is below certain threshold values, but the lipid−protein interaction reverses the domain separation behavior to make the cargo distribution homogeneous at anchor density higher than the threshold value. We conclude that the cooperative phase separation and cargo crowding-induced steric pressure are at a tug of war, and at a high enough cargo protein density on the membranes, steric pressure is dominant, far outweighing the contribution from the interaction for cooperative phase separation. Future studies may include more rigorous theoretical studies on our hypothetical model, comparative studies of protein systems with different phase behaviors, such as proteins forming nonfluidic domains, and structural study on the final outcome of cargo molecules under different conditions.

MATERIALS AND METHODS

GUV Preparation. Individual lipid mixtures were prepared by gentle hydration for each experiment's variation,[71] both homogeneous and phase-separated at 2.5, 5, and 10% concentrations of Ni-DGS and more. These mixtures were stored at −20 °C until needed. Approximately 100 μL of the lipid mixture of ∼2 mg/mL concentration was deposited in a round-bottom flask. Clean nitrogen gas was used for 5 min to remove the chloroform. The round-bottom flask was placed in a vacuum chamber for 1 hour to further dry the sample at room temperature. One milliliter of sucrose solution, with a concentration of 340 mM, was added to the round-bottom flask. The sample was incubated overnight at 38 °C. After the incubation, the newly formed GUVs were centrifuged for 15 min at 12,000*g* at room temperature. The supernatant was collected and stored at 4 °C for the experiment. Lipids were purchased from Avanti Polar Lipids Inc. (Birmingham, AL).

GUV-Protein Sample Preparation for Imaging. A stainless steel chamber was used to contain the sample for the experiment. The pieces from the assembling unit were cleaned by bath sonication for 30 min in a 1% detergent solution (Alconox, White Plains, NY), rinsed with ion-exchange filtered water, and cleaned one more time by sonication in a 1:1 solution of isopropyl alcohol and water for 30 min. Circular cover glass slides (Thermo Fisher Scientific, Waltham, MA) were cleaned by sonication in a 1:1 solution of isopropyl alcohol and water for 15 min. The pieces were assembled, and excess moisture was dried with clean nitrogen gas. A circular silicone spacer was used to narrow the sample space when needed. A bovine serum albumin solution consisting of 1 mg/mL was added for 30 min to block the glass surface. After incubation, the chamber was washed thrice with Hepes buffer solution (20 mM Hepes, 150 mM NaCl, pH 7.4).

Buffer solution and ∼1 μL of the GUV solution were added to the chamber to analyze the sample. Several *z*-stack images were acquired to assess the integrity of the GUV. Proteins were added and incubated sequentially to reach the concentration specified for each experiment, typically about 1 μM. The sample was left incubating for 1 h while a time lapse was collected to monitor the change for each step. The sample was closely monitored to ensure that the vesicles were intact and that proteins evenly interacted. After the incubation time, several *z*-stack images were acquired to analyze the end results assuming equilibrium was reached.

Fluorescence Imaging Conditions. A Nikon Ti2E-based inverted epifluorescence microscope system (Nikon, Japan) was used for imaging. A light-emitting diode (LED) white light excitation source (Lumencor, Beaverton, OR) was optically filtered with multiple optical filters and dichroic mirrors to excite and collect fluorescence emission from Atto488/GFP and Texas Red, respec-

https://doi.org/10.1021/acs.langmuir.2c00247
Langmuir 2022, 38, 4702−4712

tively. The Nikon Apo 100X TIRF oil objective with a numerical aperture of 1.49 was used for imaging. Single-molecule sensitivity with a high quantum yield sCMOS camera was used for data collection (Hamamatsu ORCA Flash 4.0, Hamamatsu, Japan). Automatic z position control was used for precise z-stack acquisition, and x, y were controlled manually. Micromanager was used to control the devices, and FIJI (ImageJ) was used for image analysis. All data collection was performed on a vibration isolation table.

Protein Purification. Most proteins used in this research were purified by *Escherichia coli* overexpression following the suggested overexpression condition from the original manuscript that each contract was developed. Centrifugally harvested *E. coli* were homogenized using the French press (Glen Mills, Clifton, NJ). After further centrifugal cleaning of heavy debris, a series of chromatography were performed, including Ni-NTA or GST affinity purification and gel filtration (Superdex 200, GE Healthcare, Chicago, IL) at 4 °C using the automated, fast chromatography system. For proteins that required removing the affinity tag, such as polyPRM, overnight enzymatic digestion at 4 °C was followed by another round of column purification. Purified proteins were characterized by SDS-PAGE (Biorad) and Nanodrop (Thermo Fisher Scientific, Waltham, MA) spectrophotometer for the 280 nm UV absorption measurement. Michael Rosen gave the polySIM−SUMO protein plasmids (Addgene plasmid #127093, #126946, and #127093),[44] and GRB2 and SOS1 protein plasmids were given by Ron Vale (Addgene plasmid #XSB363, #XSB364).[51] GST tag of the GRB2 in this report was not removed, which did not frustrate the property of LLPS. GST tag of SOS1 was enzymatically cleaved. LAT peptide was synthesized by Biomatik (Wilmington, DE). Its sequence is given in the previous report.[1] Two phosphate groups were introduced as part of the synthesis process. OregonGrenn488-malemide (Thermo Fisher Scientific, Waltham, MA) was labeled by a cysteine residue with high concentration dye incubation followed by desalting column purification (GE Healthcare, Chicago, IL). Proteins and peptides were all frozen at −80 °C until used.

■ ASSOCIATED CONTENT

Supporting Information

The Supporting Information is available free of charge at https://pubs.acs.org/doi/10.1021/acs.langmuir.2c00247.

Additional fluorescence images, Ising model simulation results (Figures S1−S5), and supporting method for additional experimental details and simulation method (PDF)

■ AUTHOR INFORMATION

Corresponding Author

Il-Hyung Lee − *Department of Chemistry and Biochemistry, Montclair State University, Montclair, New Jersey 07043, United States;* orcid.org/0000-0001-6755-3257; Email: leei@montclair.edu

Authors

Juan Ureña − *Department of Chemistry and Biochemistry, Montclair State University, Montclair, New Jersey 07043, United States*

Ashlynn Knight − *Department of Biology, Montclair State University, Montclair, New Jersey 07043, United States*

Complete contact information is available at: https://pubs.acs.org/10.1021/acs.langmuir.2c00247

Author Contributions

Conceptualization and design of the project, I.-H.L.; experimental data collection, J.U. and A.K.; data analysis, J.U. and A.K.; writing the original manuscript, I.-H.L. and J.U.; and reviewing and editing the manuscript, I.-H.L., J.U., and A.K.

Funding

The study was supported by the startup fund from the College of Science and Mathematics, Montclair State University. The study was also supported by the Garden State-Louis Stokes Alliance for Minority Participation (GS-LSAMP) scholar award program (NSF 1909824) and Student Faculty Scholarship program by the Montclair State University.

Notes

The authors declare no competing financial interest.

■ ACKNOWLEDGMENTS

The authors would like to thank Dr. Laying Wu of the Microscopy and Microanalysis Research Laboratory at Montclair State University for the microscope training and facility maintenance. A.K. acknowledges the support from the GS-LSAMP scholar awards.

■ ABBREVIATIONS

DOPC: 1,2-dioleoyl-*sn*-glycero-3-phosphocholine
DPPC: 1,2-dipalmitoyl-*sn*-glycero-3-phosphocholine
GFP: green fluorescence protein
GUV: giant unilamellar vesicle
LAT: linker for activation of T-cells
LLPS: liquid−liquid phase separation
GRB2: growth factor receptor-bound protein 2
SOS1: son of sevenless 1
Ni-DGS: 1,2-dioleoyl-*sn*-glycero-3-[(*N*-(5-amino-1-carboxypentyl)iminodiacetic acid)succinyl]
SIM: SUMO interacting motif
SUMO: small ubiquitin-like modifier
TR-DHPE: Texas Red-1,2-dihexadecanoyl-*sn*-glycero-3-phosphoethanolamine

■ REFERENCES

(1) Lee, I.-H.; Imanaka, M. Y.; Modahl, E. H.; Torres-Ocampo, A. P. Lipid raft phase modulation by membrane-anchored proteins with inherent phase separation properties. *ACS Omega* **2019**, *4*, 6551−6559.

(2) Lee, I.-H.; Kai, H.; Carlson, L.-A.; Groves, J. T.; Hurley, J. H. Negative membrane curvature catalyzes nucleation of endosomal sorting complex required for transport (ESCRT)-III assembly. *Proc. Natl. Acad. Sci. U.S.A.* **2015**, *112*, 15892−15897.

(3) Schöneberg, J.; Pavlin, M. R.; Yan, S.; Righini, M.; Lee, I.-H.; Carlson, L.-A.; Bahrami, A. H.; Goldman, D. H.; Ren, X.; Hummer, G.; Bustamante, C.; Hurley, J. H. ATP-dependent force generation and membrane scission by ESCRT-III and Vps4. *Science* **2018**, *362*, 1423−1428.

(4) Chan, Y.-H. M.; Boxer, S. G. Model membrane systems and their applications. *Curr. Opin. Chem. Biol.* **2007**, *11*, 581−587.

(5) Cohen, Z. R.; Cornell, C. E.; Catling, D. C.; Black, R. A.; Keller, S. L. Prebiotic protocell membranes retain encapsulated contents during flocculation, and phospholipids preserve encapsulation during dehydration. *Langmuir* **2022**, *38*, 1304−1310.

(6) Sugiyama, H.; Osaki, T.; Takeuchi, S.; Toyota, T. Role of negatively charged lipids achieving rapid accumulation of water-soluble molecules and macromolecules into cell-sized liposomes against a concentration gradient. *Langmuir* **2022**, *38*, 112−121.

(7) Kakimoto, Y.; Tachihara, Y.; Okamoto, Y.; Miyazawa, K.; Fukuma, T.; Tero, R. Morphology and physical properties of hydrophilic-polymer-modified lipids in supported lipid bilayers. *Langmuir* **2018**, *34*, 7201−7209.

(8) Xia, Y.; Jang, H.-S.; Shen, Z.; Bothun, G. D.; Li, Y.; Nieh, M.-P. Effects of membrane defects and polymer hydrophobicity on networking kinetics of vesicles. *Langmuir* **2017**, *33*, 5745−5751.

(9) Nielsen, J. E.; Lund, R. Molecular Transport and Growth of Lipid Vesicles Exposed to Antimicrobial Peptides. *Langmuir* **2022**, *38*, 374−384.
(10) Deplazes, E.; Tafalla, B. D.; Murphy, C.; White, J.; Cranfield, C. G.; Garcia, A. Calcium ion binding at the lipid−water interface alters the ion permeability of phospholipid bilayers. *Langmuir* **2021**, *37*, 14026−14033.
(11) Arribas Perez, M.; Beales, P. A. Biomimetic curvature and tension-driven membrane fusion induced by silica nanoparticles. *Langmuir* **2021**, *37*, 13917−13931.
(12) Sahu, A. K.; Mishra, A. K. Interaction of dopamine with zwitterionic DMPC and anionic DMPS multilamellar vesicle membranes. *Langmuir* **2021**, *37*, 13430−13443.
(13) Anselmo, S.; Sancataldo, G.; Nielsen, H. M.; Foderà, V.; Vetri, V. Peptide−membrane interactions monitored by fluorescence lifetime imaging: a study case of Transportan 10. *Langmuir* **2021**, *37*, 13148−13159.
(14) Oroojalian, F.; Beygi, M.; Baradaran, B.; Mokhtarzadeh, A.; Shahbazi, M.-A. Immune cell membrane-coated biomimetic nanoparticles for targeted cancer therapy. *Small* **2021**, *17*, No. 2006484.
(15) Pattni, B. S.; Chupin, V. V.; Torchilin, V. P. New Developments in liposomal drug delivery. *Chem. Rev.* **2015**, *115*, 10938−10966.
(16) Lei, B.; Sun, M.; Chen, M.; Xu, S.; Liu, H. ph and temperature double-switch hybrid micelles for controllable drug release. *Langmuir* **2021**, *37*, 14628−14637.
(17) Feigenson, G. W. Phase behavior of lipid mixtures. *Nat. Chem. Biol.* **2006**, *2*, 560−563.
(18) Veatch, S. L.; Keller, S. L. Separation of liquid phases in giant vesicles of ternary mixtures of phospholipids and cholesterol. *Biophys. J.* **2003**, *85*, 3074−3083.
(19) Honerkamp-Smith, A. R.; Veatch, S. L.; Keller, S. L. An introduction to critical points for biophysicists; observations of compositional heterogeneity in lipid membranes. *Biochim. Biophys. Acta, Biomembr.* **2009**, *1788*, 53−63.
(20) Lingwood, D.; Simons, K. Lipid rafts as a membrane-organizing principle. *Science* **2010**, *327*, 46−50.
(21) Cornell, C. E.; Mileant, A.; Thakkar, N.; Lee, K. K.; Keller, S. L. Direct imaging of liquid domains in membranes by cryo-electron tomography. *Proc. Natl. Acad. Sci. U.S.A.* **2020**, *117*, 19713−19719.
(22) Baumgart, T.; Hammond, A. T.; Sengupta, P.; Hess, S. T.; Holowka, D. A.; Baird, B. A.; Webb, W. W. Large-scale fluid/fluid phase separation of proteins and lipids in giant plasma membrane vesicles. *Proc. Natl. Acad. Sci. U.S.A.* **2007**, *104*, 3165−3170.
(23) Johnson, S. A.; Stinson, B. M.; Go, M. S.; Carmona, L. M.; Reminick, J. I.; Fang, X.; Baumgart, T. Temperature-dependent phase behavior and protein partitioning in giant plasma membrane vesicles. *Biochim. Biophys. Acta, Biomembr.* **2010**, *1798*, 1427−1435.
(24) Veatch, S. L.; Cicuta, P.; Sengupta, P.; Honerkamp-Smith, A.; Holowka, D.; Baird, B. Critical fluctuations in plasma membrane vesicles. *ACS Chem. Biol.* **2008**, *3*, 287−293.
(25) Eggeling, C.; Ringemann, C.; Medda, R.; Schwarzmann, G.; Sandhoff, K.; Polyakova, S.; Belov, V. N.; Hein, B.; von Middendorff, C.; Schönle, A.; Hell, S. W. Direct observation of the nanoscale dynamics of membrane lipids in a living cell. *Nature* **2009**, *457*, 1159−1162.
(26) Frisz, J. F.; Lou, K.; Klitzing, H. A.; Hanafin, W. P.; Lizunov, V.; Wilson, R. L.; Carpenter, K. J.; Kim, R.; Hutcheon, I. D.; Zimmerberg, J.; Weber, P. K.; Kraft, M. L. Direct chemical evidence for sphingolipid domains in the plasma membranes of fibroblasts. *Proc. Natl. Acad. Sci. U.S.A.* **2013**, *110*, E613−E622.
(27) Shelby, S. A.; Castello-Serrano, I.; Wisser, K. C.; Levental, I.; Veatch, S. L. Membrane phase separation drives organization at B cell receptor clusters. *bioRxiv* 2021, DOI: 10.1101/2021.05.12.443834.
(28) Kenworthy, A. K.; Petranova, N.; Edidin, M. High-Resolution FRET microscopy of cholera toxin B-subunit and GPI-anchored proteins in cell plasma membranes. *Mol. Biol. Cell* **2000**, *11*, 1645−1655.
(29) Rayermann, S. P.; Rayermann, G. E.; Cornell, C. E.; Merz, A. J.; Keller, S. L. Hallmarks of reversible separation of living, unperturbed cell membranes into two liquid phases. *Biophys. J.* **2017**, *113*, 2425−2432.
(30) Toulmay, A.; Prinz, W. A. Direct imaging reveals stable, micrometer-scale lipid domains that segregate proteins in live cells. *J. Cell Biol.* **2013**, *202*, 35−44.
(31) Levental, I.; Levental, K. R.; Heberle, F. A. Lipid rafts: controversies resolved, mysteries remain. *Trends Cell Biol.* **2020**, *30*, 341−353.
(32) Pike, L. J. Rafts defined: a report on the Keystone symposium on lipid rafts and cell function. *J. Lipid Res.* **2006**, *47*, 1597−1598.
(33) Takeda, M.; Leser, G. P.; Russell, C. J.; Lamb, R. A. Influenza virus hemagglutinin concentrates in lipid raft microdomains for efficient viral fusion. *Proc. Natl. Acad. Sci. U.S A.* **2003**, *100*, 14610−14617.
(34) Cheng, H.; Vetrivel, K. S.; Gong, P.; Meckler, X.; Parent, A.; Thinakaran, G. Mechanisms of Disease: new therapeutic strategies for Alzheimer's disease−targeting APP processing in lipid rafts. *Nat. Clin. Pract. Neurol.* **2007**, *3*, 374−382.
(35) Filipp, D.; Leung, B. L.; Zhang, J.; Veillette, A.; Julius, M. Enrichment of lck in lipid rafts regulates colocalized fyn activation and the initiation of proximal signals through TCR alpha beta. *J. Immunol.* **2004**, *172*, 4266−4274.
(36) Raghu, H.; Sodadasu, P. K.; Malla, R. R.; Gondi, C. S.; Estes, N.; Rao, J. S. Localization of upar and MMP-9 in lipid rafts is critical for migration, invasion and angiogenesis in human breast cancer cells. *BMC Cancer* **2010**, *10*, No. 647.
(37) Lorent, J. H.; Diaz-Rohrer, B.; Lin, X.; Spring, K.; Gorfe, A. A.; Levental, K. R.; Levental, I. Structural determinants and functional consequences of protein affinity for membrane rafts. *Nat. Commun.* **2017**, *8*, No. 1219.
(38) Diaz-Rohrer, B. B.; Levental, K. R.; Simons, K.; Levental, I. Membrane raft association is a determinant of plasma membrane localization. *Proc. Natl. Acad. Sci. U.S.A.* **2014**, *111*, 8500−8505.
(39) Zacharias, D. A.; Violin, J. D.; Newton, A. C.; Tsien, R. Y. Partitioning of lipid-modified monomeric gfps into membrane microdomains of live cells. *Science* **2002**, *296*, 913−916.
(40) Li, P.; Banjade, S.; Cheng, H.-C.; Kim, S.; Chen, B.; Guo, L.; Llaguno, M.; Hollingsworth, J. V.; King, D. S.; Banani, S. F.; Russo, P. S.; Jiang, Q.-X.; Nixon, B. T.; Rosen, M. K. Phase transitions in the assembly of multivalent signalling proteins. *Nature* **2012**, *483*, 336−340.
(41) Boeynaems, S.; Alberti, S.; Fawzi, N. L.; Mittag, T.; Polymenidou, M.; Rousseau, F.; Schymkowitz, J.; Shorter, J.; Wolozin, B.; Van Den Bosch, L.; Tompa, P.; Fuxreiter, M. Protein Phase Separation: A New Phase in Cell Biology. *Trends Cell Biol.* **2018**, *28*, 420−435.
(42) Lin, Y.; Currie, S. L.; Rosen, M. K. Intrinsically disordered sequences enable modulation of protein phase separation through distributed tyrosine motifs. *J. Biol. Chem.* **2017**, *292*, 19110−19120.
(43) Wang, J.; Choi, J.-M.; Holehouse, A. S.; Lee, H. O.; Zhang, X.; Jahnel, M.; Maharana, S.; Lemaitre, R.; Pozniakovsky, A.; Drechsel, D.; Poser, I.; Pappu, R. V.; Alberti, S.; Hyman, A. A. A Molecular Grammar Governing the Driving Forces for Phase Separation of Prion-like RNA Binding Proteins. *Cell* **2018**, *174*, 688−699.e16.
(44) Banani, S. F.; Rice, A. M.; Peeples, W. B.; Lin, Y.; Jain, S.; Parker, R.; Rosen, M. K. Compositional Control of Phase-Separated Cellular Bodies. *Cell* **2016**, *166*, 651−663.
(45) Schuster, B. S.; Reed, E. H.; Parthasarathy, R.; Jahnke, C. N.; Caldwell, R. M.; Bermudez, J. G.; Ramage, H.; Good, M. C.; Hammer, D. A. Controllable protein phase separation and modular recruitment to form responsive membraneless organelles. *Nat. Commun.* **2018**, *9*, No. 2985.
(46) Brangwynne, C. P.; Eckmann, C. R.; Courson, D. S.; Rybarska, A.; Hoege, C.; Gharakhani, J.; Jülicher, F.; Hyman, A. A. Germline P granules are liquid droplets that localize by controlled dissolution/condensation. *Science* **2009**, *324*, 1729−1732.
(47) Wheeler, J. R.; Matheny, T.; Jain, S.; Abrisch, R.; Parker, R. Distinct stages in stress granule assembly and disassembly. *eLife* **2016**, *5*, No. e18413.

(48) Riback, J. A.; Zhu, L.; Ferrolino, M. C.; Tolbert, M.; Mitrea, D. M.; Sanders, D. W.; Wei, M.-T.; Kriwacki, R. W.; Brangwynne, C. P. Composition-dependent thermodynamics of intracellular phase separation. *Nature* **2020**, *581*, 209−214.
(49) Huang, W. Y. C.; Alvarez, S.; Kondo, Y.; Lee, Y. K.; Chung, J. K.; Lam, H. Y. M.; Biswas, K. H.; Kuriyan, J.; Groves, J. T. A molecular assembly phase transition and kinetic proofreading modulate Ras activation by SOS. *Science* **2019**, *363*, 1098−1103.
(50) Huang, W. Y. C.; Yan, Q.; Lin, W.-C.; Chung, J. K.; Hansen, S. D.; Christensen, S. M.; Tu, H.-L.; Kuriyan, J.; Groves, J. T. Phosphotyrosine-mediated LAT assembly on membranes drives kinetic bifurcation in recruitment dynamics of the Ras activator SOS. *Proc. Natl. Acad. Sci. U.S.A.* **2016**, *113*, 8218−8223.
(51) Su, X.; Ditlev, J. A.; Hui, E.; Xing, W.; Banjade, S.; Okrut, J.; King, D. S.; Taunton, J.; Rosen, M. K.; Vale, R. D. Phase separation of signaling molecules promotes T cell receptor signal transduction. *Science* **2016**, *352*, 595−599.
(52) Hosokawa, T.; Liu, P.-W.; Cai, Q.; Ferreira, J. S.; Levet, F.; Butler, C.; Sibarita, J.-B.; Choquet, D.; Groc, L.; Hosy, E.; Zhang, M.; Hayashi, Y. camkii activation persistently segregates postsynaptic proteins via liquid phase separation. *Nat. Neurosci.* **2021**, *24*, 777−785.
(53) Chen, X.; Wu, X.; Wu, H.; Zhang, M. Phase separation at the synapse. *Nat. Neurosci.* **2020**, *23*, 301−310.
(54) Banjade, S.; Rosen, M. K. Phase transitions of multivalent proteins can promote clustering of membrane receptors. *eLife* **2014**, *3*, No. e04123.
(55) Beutel, O.; Maraspini, R.; Pombo-García, K.; Martin-Lemaitre, C.; Honigmann, A. Phase separation of zonula occludens proteins drives formation of tight junctions. *Cell* **2019**, *179*, 923−936.e11.
(56) Chung, J. K.; Huang, W. Y. C.; Carbone, C. B.; Nocka, L. M.; Parikh, A. N.; Vale, R. D.; Groves, J. T. Coupled membrane lipid miscibility and phosphotyrosine-driven protein condensation phase transitions. *Biophys. J.* **2021**, *120*, 1257−1265.
(57) Goh, S. L.; Amazon, J. J.; Feigenson, G. W. Toward a better raft model: modulated phases in the four-component bilayer, DSPC/DOPC/POPC/CHOL. *Biophys. J.* **2013**, *104*, 853−862.
(58) Baumgart, T.; Hunt, G.; Farkas, E. R.; Webb, W. W.; Feigenson, G. W. Fluorescence probe partitioning between Lo/Ld phases in lipid membranes. *Biochim. Biophys. Acta, Biomembr.* **2007**, *1768*, 2182−2194.
(59) Ditlev, J. A.; Case, L. B.; Rosen, M. K. Who's In and Who's Out−Compositional Control of Biomolecular Condensates. *J. Mol. Biol.* **2018**, *430*, 4666−4684.
(60) Scheve, C. S.; Gonzales, P. A.; Momin, N.; Stachowiak, J. C. Steric pressure between membrane-bound proteins opposes lipid phase separation. *J. Am. Chem. Soc.* **2013**, *135*, 1185−1188.
(61) Imam, Z. I.; Kenyon, L. E.; Carrillo, A.; Espinoza, I.; Nagib, F.; Stachowiak, J. C. Steric pressure among membrane-bound polymers opposes lipid phase separation. *Langmuir* **2016**, *32*, 3774−3784.
(62) Houser, J. R.; Hayden, C. C.; Thirumalai, D.; Stachowiak, J. C. A Förster resonance energy transfer-based sensor of steric pressure on membrane surfaces. *J. Am. Chem. Soc.* **2020**, *142*, 20796−20805.
(63) Berry, J.; Brangwynne, C. P.; Haataja, M. Physical principles of intracellular organization via active and passive phase transitions. *Rep. Prog. Phys.* **2018**, *81*, No. 046601.
(64) Stanich, C. A.; Honerkamp-Smith, A. R.; Putzel, G. G.; Warth, C. S.; Lamprecht, A. K.; Mandal, P.; Mann, E.; Hua, T.-A. D.; Keller, S. L. Coarsening dynamics of domains in lipid membranes. *Biophys. J.* **2013**, *105*, 444−454.
(65) Shin, Y.; Brangwynne, C. P. Liquid phase condensation in cell physiology and disease. *Science* **2017**, *357*, No. eaaf4382.
(66) Dignon, G. L.; Zheng, W.; Kim, Y. C.; Mittal, J. Temperature-controlled liquid−liquid phase separation of disordered proteins. *ACS Cent. Sci.* **2019**, *5*, 821−830.
(67) Cinar, H.; Fetahaj, Z.; Cinar, S.; Vernon, R. M.; Chan, H. S.; Winter, R. H. A. Temperature, hydrostatic pressure, and osmolyte effects on liquid−liquid phase separation in protein condensates: physical chemistry and biological implications. *Chem. - Eur. J.* **2019**, *25*, 13049−13069.
(68) Möller, J.; Grobelny, S.; Schulze, J.; Bieder, S.; Steffen, A.; Erlkamp, M.; Paulus, M.; Tolan, M.; Winter, R. Reentrant liquid-liquid phase separation in protein solutions at elevated hydrostatic pressures. *Phys. Rev. Lett.* **2014**, *112*, No. 028101.
(69) Rouches, M.; Veatch, S. L.; Machta, B. B. Surface densities prewet a near-critical membrane. *Proc. Natl. Acad. Sci. U.S.A.* **2021**, *118*, No. e2103401118.
(70) Gu, R.-X.; Baoukina, S.; Tieleman, D. P. Phase separation in atomistic simulations of model membranes. *J. Am. Chem. Soc.* **2020**, *142*, 2844−2856.
(71) Reeves, J. P.; Dowben, R. M. Formation and properties of thin-walled phospholipid vesicles. *J. Cell. Physiol.* **1969**, *73*, 49−60.

https://doi.org/10.1021/acs.langmuir.2c00247
Langmuir 2022, 38, 4702−4712